Interaction of atomic hydrogen with anthracene and polyacene from density functional theory

Ricardo M. Ferullo [a],[*], Norberto J. Castellani [b], Patricia G. Belelli [b]

[a] INQUISUR, CONICET and Universidad Nacional del Sur, Av. Alem 1253, 8000 Bahía Blanca, Argentina
[b] IFISUR, CONICET and Universidad Nacional del Sur, Av. Alem 1253, 8000 Bahía Blanca, Argentina

ABSTRACT

The interaction of atomic hydrogen with two linear polycyclic aromatic hydrocarbons (PAHs), anthracene and polyacene (the polymer of benzene), was studied within the density functional theory (DFT). Using a proper dispersion-corrected method (DFT-D) the preferential physisorption sites were explored. The activation barrier for the bond formation between a peripheral C and the incoming H was calculated to be 58.5 and 34.1 meV with pure DFT on anthracene and polyacene at its antiferromagnetic ground state, respectively. DFT-D, although improves the description of the physisorbed state, tends to underestimate the chemisorption barriers due an artifact arising from the dispersion correction.

© 2016 Elsevier B.V. All rights reserved.

1. Introduction

The study of polycyclic aromatic hydrocarbons (PAHs) is of great interest in different technological and academic areas. In environmental sciences, it is attractive because PAH molecules are pollutant gases present in the air, most of them produced by the burning of hydrocarbon based fuels [1]; in this context, the formation of soot particles from clustering and the reactions involving PAH molecules are topics that are receiving increasing attention [2–5]. Furthermore, PAH molecules may possibly be used for components in nanoelectronic devices [6]. In astrochemistry, it was proposed that PAHs could be an important component of interstellar dust, accounting for a series of detected infrared emission bands [7]; in diffuse cloud environments PAHs are thought to exist in the gas phase, while in dense clouds both gas and condensed phase of PAHs are expected [8].

It is generally accepted that molecular hydrogen, H_2, the most abundant molecule in the Universe, is catalytically formed from atomic hydrogen on the surface of dust grains present in the interstellar medium (ISM) [9]. H atoms can be physisorbed in these conditions because the temperature is low enough to prevent desorption ($T \leq 40$ K) from the shallow physisorption well. Graphite and graphene surfaces have been used in the past to simulate the H interaction and further H_2 formation occurring on dust grains in the ISM [10–15]. However, new proposals suggest that PAH molecules could act as catalytic centers for the formation of H_2

[16–23]. According to this model, firstly a H atom coming from gas phase is captured by a PAH molecule by forming a C—H chemical bond; then, this hydrogen is abstracted by a second H atom, thus forming the H_2 molecule.

Atomic hydrogen binds preferentially at the edges of PAHs [18,19,24]. Density functional (DFT) calculations indicate that the addition of the first H atom requires a barrier of about 60 meV to the coronene molecule [18]. However, subsequent addition reactions have small or vanishing barrier, indicating that the efficiency of PAHs to catalyze molecular hydrogen depends on the degree of hydrogenation. From that, a catalytic cycle of hydrogen addition and abstraction reactions leading H_2 was proposed. In the case of the coronene molecule, once more than three excess H atoms are added to the neutral molecule it will act as a catalyst for H_2 formation with vanishing effective reaction barriers [18]. Interestingly, a barrier of also 60 meV for the addition of the first H on pyrene for the most reactive channel was also obtained using DFT [19]. On the other hand, it was experimentally observed that UV radiation promotes the ejection of H_2 from hydrogenated PAHs [17]. Using coronene films, Mennella et al., [20] have observed the hydrogenation of the outer edge C atoms and the exchange reaction on these sites, with the formation of H_2 via the Eley–Rideal (ER) mechanism.

A type of PAHs that has attracted increasing interest is the so-called graphene nanoribbons (GNR). They can be considered as strips of graphene with ultra-thin width. It has been theoretically shown that the ground state of infinitely extended zigzag-edged graphene nanoribbons (ZGNR) is the antiferromagnetic (AFM) phase, with one edge spin up and the other spin down [4,25]. In the less stable ferromagnetic (FM) phase the spins at the two edges are all up. It has been demonstrated that at its AFM state,

* Corresponding author.
E-mail address: caferull@criba.edu.ar (R.M. Ferullo).

spin-polarized π electrons are localized on the zigzag C atoms in such a way that on average each edge C atom has a local magnetic moment of about 0.14 μ_B [4]. Due to this 'partial radical' character, these edge C atoms have unique chemical reactivity, comparing with non-edge C atoms, armchair-edge GNRs, small PAHs, or nanotube carbon atoms, which show little or no radical character [4]. Density functional theory simulations predict that antiferromagnetic ZGNRs should be stable only at very low pressures [26].

Interestingly, 'rectangular' molecules of PAHs containing only 11 aromatic rings already present magnetism with AFM state more stable than FM [27]. More specifically, as the PAH increases the side of the rectangle greater than 3 rings, a stable AFM phase appears. Also here, the AFM phase arises from the zigzag edges. These findings firstly predicted by density functional theory were recently supported by more sophisticated multireference methods [28].

Among the different types of quasi-one-dimensional PAHs, acenes (linearly fused benzene rings) have aroused particular attention [25,29,30]. It was shown from DFT that the ground state of higher acenes (from eight benzene rings) is the AFM phase as well. Conversely, for shorter acenes the ground state is predicted to be the non-magnetic phase (NM) [25].

The main objectives of this work are: (i) studying by means of an appropriate DFT approach the physical interaction of atomic H with anthracene and polyacene. (ii) Analyzing the activation barrier on a prototype zigzag-ended PAHs which present partial radical character, i.e., some degree of local magnetism. This kind of active site is expected to be present in relatively large PAHs, molecules that, as previously mentioned, can show a particular chemical reactivity. For this purpose, an infinitely extended chain of aromatic rings (polyacene) was modeled. For comparison, the simple PAH molecule of anthracene was used as a model of molecule in which magnetism is absent. It is interesting to mention that anthracene and long acenes have been investigated in relation to their possible existence in the ISM [22,31,32]. We have chosen the polyacene molecule because it is simple to model using a periodic approach, in comparison with long n-acenes or rectangular PAHs with multiradical character which are formed at least by around 10 aromatic rings [27]. We focus our attention particularly on the 'physisorption' state, since it is expected that this weak interaction can take place at low temperature conditions than those present in the ISM. Furthermore, it is interesting to know if it is possible to obtain, from the general perspective of DFT, a sufficiently accurate description of the whole process for the H interaction with PAHs, i.e., physisorption, activation barrier and chemisorption. Notice that we adopt a surface science terminology, whereby 'physisorption' and 'chemisorption' are used interchangeably with 'chemical binding' and 'physical binding' to the molecule, respectively.

2. Method

A precise description of dispersion interactions is in general a challenging task for quantum-chemical methods. Nowadays, density functional theory (DFT) has becomes a widely used method to study complex molecular systems because of its accuracy, computational feasibility and versatility. However, currently available DFT functionals fail in describing non-covalent interactions such as dispersion or van der Waals (vdW) forces. Since H physisorption on PAHs is dominated by dispersion forces, the method employed in the present study requires a very good description to this type of long-range interactions. Here we have used an empirical correction to account for vdW interactions. As we shall see below this approach resulted to be more appropriate than others in which dispersion forces are treated from first-principles.

DFT calculations were performed using the Vienna Ab Initio Simulation Package (VASP) [33–35]. In this code, the Kohn-Sham

equations are solved employing plane wave bases and periodic boundary conditions. For benzene and anthracene, a large box of $25 \times 25 \times 25 \, \text{Å}^3$ was adopted and only the Gamma point was used to sample the Brillouin zone. For polyacene, the unit cell is shown in Fig. 1. This ideal infinite polymer is separated by its periodic images by a 20-Å vacuum layer along y- and z-directions, and 7 k-points were employed to sample the one-dimensional irreducible Brillouin zone. A kinetic energy cutoff of 500 eV was used. All the atoms were allowed to relax until forces on them were smaller than 10^{-4} eV/Å.

Preliminary tests for the H physisorption on benzene and anthracene at hollow sites were performed using second-order Møller-Plesset (MP2) calculations using the Gaussian-03 code [36]. Dunning-type correlation-consistent polarized valence triple basis sets augmented with one diffuse function (aug-cc-pVTZ) was used. The MP2 results have been used as a reference to test the performance of the different DFT functionals.

Three dispersion-corrected DFT were employed. The first one is an R^{-6} empirical correction, usually denoted as DFT-D. In this approach, the total energy is given by

$$E_{\text{DFT-D}} = E_{\text{DFT}} + E_{\text{disp}} \tag{1}$$

where E_{DFT} is the Kohn–Sham total energy as obtained from genuine PBE and E_{disp} is an empirical dispersion correction given by

$$E_{\text{disp}} = -s_6 \sum_{i,j} f(R_{ij}) C_6^{ij} (R_{ij})^{-6} \tag{2}$$

where $f(R_{ij})$ represents a damping function and the C_6^{ij} coefficients are obtained from atomic polarizabilities and ionization potentials. On the other hand, s_6 is a scaling factor which was optimized in 0.75 for PBE [37].

The second method is based on the nonlocal functional proposed by Dion et al. [38] (vdW-DF) where the dispersion term is calculated self-consistently. Klimeš et al. [39] have developed several new functionals based from the one originally proposed by Dion et al. [38]. Among these, we have chosen the optPBE functional, which has shown that improves the interaction energies of dispersion and hydrogen bonded complexes. Hereafter, we will call 'pure' or 'standard' DFT to the generalized gradient approximation (GGA) method. Here, the calculations of this type were performed using the PBE functional.

Transition states and activation barriers (E_{act}) were calculated using the Climbing-image Nudged Elastic Band (CI-NEB) method [40] implemented in VASP. This technique allows finding the minimal energy pathway between each initial and final state pair and the corresponding transition state. The saddle points were validated as transition states with vibrational analysis by the presence of a single imaginary frequency.

The physisorption (chemisorption) energy of H atom was calculated as the following energy difference:

$$E_{\text{phys(chem)}} = -E(\text{H/molecule}) + [E(\text{molecule}) + E(\text{H})] \tag{3}$$

For MP2 calculations, basis set superposition error (BSSE) was corrected by the counterpoise procedure (CP) [41].

3. Results

As mentioned, before attacking the problem of computing the physisorption energy of atomic hydrogen on anthracene and polyacene we have performed preliminary tests on H-benzene and H-anthracene systems with the MP2 method in order to check the performance of the different vdW-corrected DFT. All these complementary calculations were carried out with the H atom above the center of the benzene molecule (hollow site) and in the same position on the central ring of anthracene (see Fig. 1).
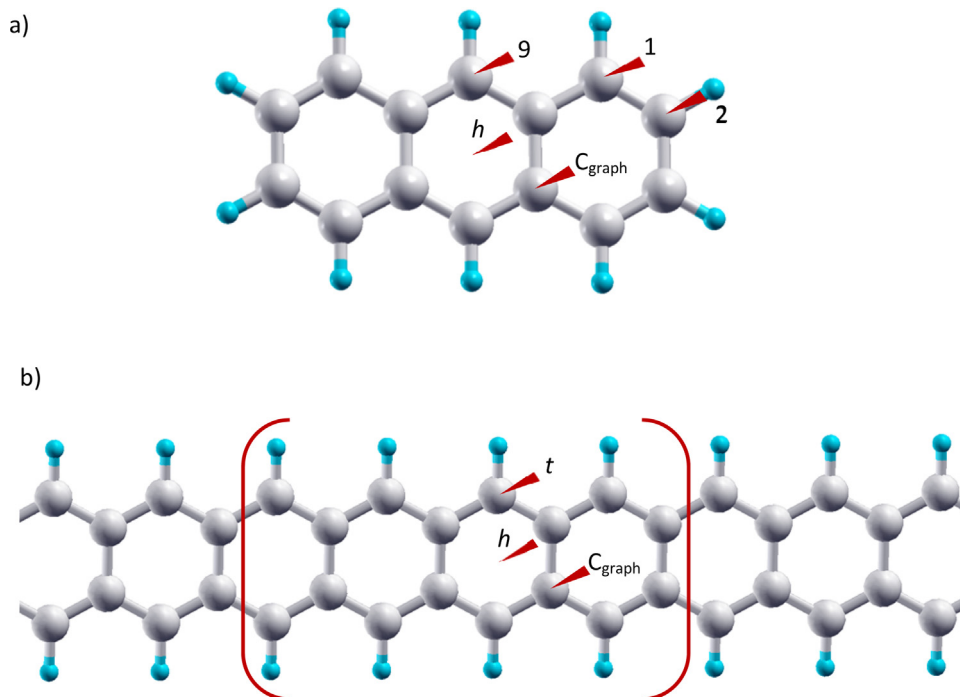
Fig. 1. Top view geometries of: (a) anthracene and (b) polyacene (h: hollow; t: top; C_{graph}: 'graphitic' C atoms). The supercell used for polyacene is enclosed in brackets. The analyzed adsorption sites are shown. On anthracene, non-equivalent top positions are labeled with numbers.

Table 1

Physisorption energy (E_{phys}, in meV) of atomic hydrogen on the hollow site of benzene; z (in Å) is the optimized perpendicular distance from the center of the benzene molecule.

Method	E_{phys}	z
DFT-D[a]	22.5	2.89
vdW-DF[a]	44.4	3.12
vdW-DF[b]	43	3.14
optPBE[a]	57.5	2.91
MP2[c]	23.6	3.02
MP2[d]	25.3	–
CCSD(T)[d]	24.8	–
DMC[b]	26	2.95
DFT (PBE)[b]	7	3.44

[a] This work. VASP calculations.
[b] Ma et al. [43].
[c] This work. GAUSSIAN calculations using aug-cc-pVTZ and BSSE-corrected.
[d] Bonfanti et al. [42], at a z fixed distance of 3.11 Å.

Table 2

Physisorption energies (E_{phys}, in meV) of atomic hydrogen on anthracene at the hollow site of the central ring using different methods; z (in Å) is the optimized perpendicular distance.

Method	E_{phys}(meV)	z
MP2	29.1	2.94
DFT-D	24.7	2.88
vdW-DF	62.2	3.02
optPBE	77.9	2.83
DFT	6.7	3.53

Our results for the H-benzene system are presented in Table 1, together with other calculations reported in the literature. Our MP2/aug-cc-pVTZ results agree well with those obtained under MP2 and CCSD(T) using a more extended basis set [42], and even with Quantum Monte Carlo simulations within the Diffusion Monte Carlo (DMC) scheme [43]. As expected, PBE largely underestimates the binding energy. Regarding the DFT-based methods, DFT-D predicts a physisorption energy which agrees fairly well with the above mentioned high-level calculations. In fact, the results are much better than in principle more refined vdW-DF and optPBE approaches. For H-anthracene, the tendencies are similar than on benzene, i.e., DFT-D performs better than using those functionals in which the dispersion term is treated self-consistently in comparison with our calculations at MP2 level (see Table 2). The DFT-D method was employed previously to study the H physisorption on coronene [10,43–45] giving values of E_{phys} in the range of 30–43 meV (according to the type of empirical approximation), in satisfactory agreement with MP2 (39.5 meV) [42] and Quantum Monte Carlo (43 meV) [43] calculations. Also in this case, when the

dispersion interaction is obtained directly from electron density the predicted physisorption energies are overestimated [43]. The good performance of DFT-D was recently observed for H_2 physisorption on coronene [46]. Considering these results, we have carried out all the calculations of physisorption using DFT-D. Results using pure DFT are also reported for comparison.

Results for the H physisorption on anthracene on top and hollow positions are presented in Table 3. Following IUPAC rules, we have labeled the non-equivalent C sites as C1, C2 and C9. The 'graphitic' C atoms, i.e., those C atoms bonded to other three C atoms are indicated as C_{graph} (Fig. 1). DFT-D results indicate that, among the on-top geometries, the preferred physisorption sites are C_{graph} and C9 with similar E_{phys} values (20.3 and 18.1 meV, respectively). The hollow site remains as the global minimum. Conversely, under DFT the physisorption energies are very low for all the studied sites, in the range of 4.5–6.7 meV.

Apart from the above-mentioned ER mechanism, H_2 can be catalytically formed in the ISM following the Langmuir–Hinshelwood (LH) mechanism, where two mobile H atoms meet and react on a surface. It is thus interesting to estimate the diffusion barriers on these PAH molecules. In Table 3 the differences of physisorption energies (ΔE_{phys}) between hollow and top sites are also shown. The ΔE_{phys} value can be considered as the minimal diffusion barrier for the mobility from hollow site to a different nearby site. The results using DFT-D for the diffusion from the hollow site to C9 or C_{graph} are 6.6 and 4.4 meV, respectively. These values are very similar than

Table 3

Physisorption energies (E_{phys}, in meV) of atomic hydrogen on different sites of anthracene and polyacene (see Fig. 1). ΔE_{phys} values are calculated as $\Delta E_{phys} = E_{phys}(\text{hollow}) - E_{phys}(\text{site})$; d_{HC} (in Å) is the distance between the incoming H and the nearest C atom.

	DFT			DFT-D		
	E_{phys}(meV)	ΔE_{phys}(meV)	d_{HC}	E_{phys}(meV)	ΔE_{phys}(meV)	d_{HC}
H-Anthracene						
Hollow	6.7	0.0	3.53	24.7	0.0	3.21
C_{graph}	5.5	1.2	3.59	20.3	4.4	3.13
C9	5.0	1.7	3.55	18.1	6.6	3.02
C1	4.8	1.9	3.57	15.5	9.2	3.10
C2	4.5	2.2	3.60	12.2	12.5	3.18
H-Polyacene (AFM)						
Hollow	5.9	0.0	3.90	25.1	0.0	3.21
C_{graph}	5.1	0.8	3.76	19.4	5.7	3.09
Top	5.6	0.3	3.56	–[a]	–	–

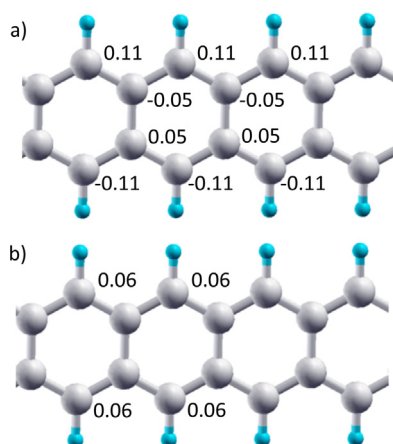[a] A barrierless chemisorption is predicted.

Fig. 2. Local magnetic moments (in μ_B): (a) for antiferromagnetic (AFM) and (b) ferromagnetic (FM) phases of polyacene. Atomic magnetic moments not shown in the figure are null or nearly null (magnitudes smaller than 0.01 μ_B).

the barriers for the migration from hollow to top sites on inner C atoms of coronene calculated at MP2 level (5 meV) [42], indicating the extremely high mobility of physisorbed H atoms.

Concerning the polyacene electronic structure, we firstly present the results of their different magnetic phases. In line with previous theoretical calculations [25], two electronic structures with multiradical character were obtained, the antiferromagnetic (AFM) and the ferromagnetic (FM) states. Our DFT calculations predict that the AFM phase is more stable than at the FM one by about 70 meV/cell. Edge C atoms of polyacene present values of 0.11/−0.11 μ_B, and of 0.06 μ_B at AFM and FM phases, respectively (Note that we call 'edge' or 'peripheral' C atoms of polyacene to those atoms linked to two C atoms and to one H atom). From the different possibilities of spin arrays with antiferromagnetism, we have considered that one in which one edge presents spin up and the other spin down (Fig. 2), although in principle, other arrangements are possible. In our model to study the H interaction with an edge C atom with partial radical character we have only used the polyacene chain in this AFM array.

In Table 3, the H physisorption energies on AFM polyacene are also reported. In our simulations, we have analyzed the physisorption taking as initial configuration that one in which the edge C atom and the incoming H atom have opposite spin orientations. Our DFT-D calculations indicate that no physisorption minimum is predicted on the edge C atom. Instead, we have observed that the energetic profile presented a plateau at around 20 meV without the formation of a defined physisorption well. As we will discuss later, this phenomenon may be caused by a spurious effect of the

dispersion correction. With respect to the other possible sites that have well defined physisorption minima, hollow resulted to be the preferred one. The minimal diffusion barrier from hollow to C_{graph} was calculated in 5.7 meV, a similar value than on anthracene.

On PAHs, it is well established [18,19] that edge C atoms are much more reactive than C_{graph} atoms. In fact, DFT calculated activation barriers are in the range of 60–120 meV for the formers and 200–270 meV for the latters (with chemisorption energies of 1.1–1.6 eV and 0.6 eV, respectively) [18,19]. In Table 4 the chemisorption (E_{chem}) and activation (E_{act}) energies of AFM polyacene and anthracene are shown, together with the already reported physisorption energies. We have only considered the position 9 of anthracene for the calculation of the entire adsorption reaction.

At DFT level the activation barrier was calculated to be 58.5 meV on anthracene, essentially the same than that obtained for pyrene and coronene [18,19]. However, when dispersion effects are explicitly included, the barrier decreases to 24.5 meV. A similar effect of the dispersion correction was previously observed on graphene and on inner C atoms of coronene [10,47]; for example, on coronene the chemisorpion barrier decreases from 0.25 (DFT) to 0.19 eV (DFT-D) [10].

The schematic reaction profiles are shown in Fig. 3. The activation barrier (E_{act}) for polyacene at the AFM state results to be 34.1 meV with DFT, and vanishes completely using DFT-D. On both anthracene and polyacene, chemisorption energies are strongly exothermic, being nearly 0.6 eV more stable on the latter.

Using DFT and high-level coupled clusters methods, Wang et al. [48] have carried out a comparative study of H chemisorption barriers on inner C atoms of pyrene and coronene as models of graphite surfaces. They observed that PBE underestimates the activation barrier with respect to the high-level calculations. Indeed, it is well-known that pure DFT approaches typically at too low energies for reaction barriers due to the self-interaction error [49].

In the DFT-D approach, as mentioned above, the incorporation of empirical corrections for dispersion forces causes a decrease of E_{act} values with respect to pure DFT results. We have to bear in mind that the empirical term (Eq. (2)) is constructed to describe correctly the asymptotic behavior of long-range dispersion interactions between two separated molecular fragments, and therefore it should be valid only in this regime. However, it is clear that it affects the whole energy profile, from the physisorption well down to the chemisorption well. At the transition state, this term provides an additional attractive energy between H and PAH, thus yielding even lower activation barriers. From these considerations, we conclude that DFT-D seems to predict worse results for chemisorption barriers than pure DFT due to an artifact arising from the used damping function. However, it remains to be seen how close standard DFT approximates to the 'exact' potential energy

Table 4
On top physisorption (in meV) and chemisorption (in eV) energies for H interaction with anthracene (on C9 site) and AFM polyacene. In parentheses, the distance between the incoming H and the C atom to which it is bonded (d_{HC}, in Å).

	DFT			DFT-D		
	E_{phys} (meV)	E_{act} (meV)	E_{chem} (eV)	E_{phys} (meV)	E_{act} (meV)	E_{chem} (eV)
Anthracene	5.0 (3.55)	58.5 (2.24)	1.94 (1.11)	18.1 (3.02)	24.5 (2.15)	1.98 (1.11)
Polyacene (AFM)	5.6 (3.56)	34.1 (2.25)	2.52 (1.11)	–[a]	0.00[a]	2.56 (1.11)

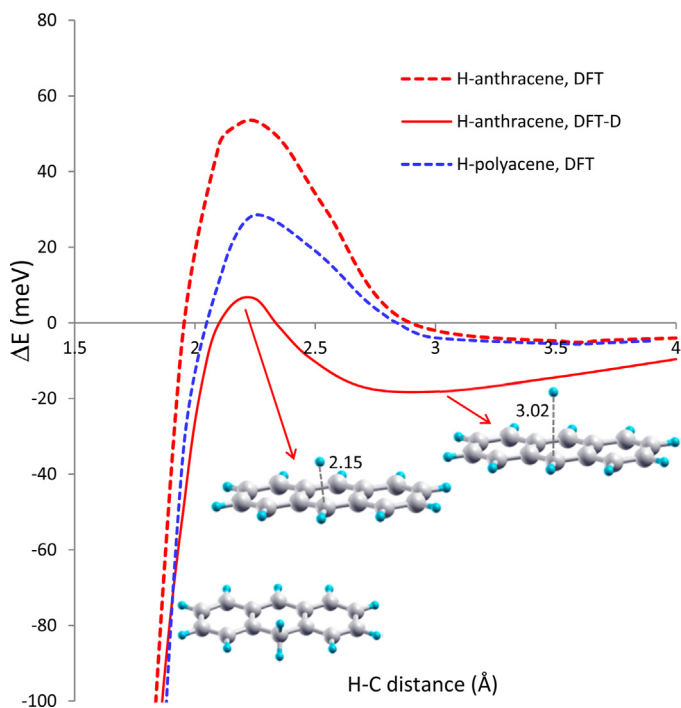[a] A barrierless chemisorption is predicted.

Fig. 3. Schematic potential energy curves showing physisorption energies and activation barriers as a function of the C–H increasing distance for H interaction with anthracene (on C9 site) and AFM polyacene. The energy values are referred to isolated species (PAH + free H atom).

Fig. 4. Local magnetic moments (in μ_B): (a) for singly hydrogenated (one additional H atom per cell) polyacene and, (b) doubly hydrogenated (two additional H atoms per cell) polyacene. For the first structure, the atomic magnetic moments not shown in the figure are null or nearly null. For doubly hydrogenated polyacene, all the atomic magnetic moments are null (non-magnetic state).

barrier for H chemisorption on edge C atoms of PAHs. It is important to observe that the accuracy of reaction barriers are in general improved when the exact Hartree–Fock exchange is mixed into the exchange-correlation energy through the hybrid-DFT functionals [48,49]; however, they also fail in the correct description of the physisorption states.

The corresponding array of atomic magnetic moments of singly hydrogenated polyacene (with one additional H atom per cell) is presented in Fig. 4. As we can see, the opposite C edge atoms present relatively large local magnetic moments, while are essentially null at the edge on which the hydrogenation is produced. In particular, the *para* position relative to the firstly hydrogenated C atom presents the highest magnetic moment. Our calculations show that a second incoming H atom interacts barrierless with this edge C yielding a non-magnetic structure (Fig. 4); in this case, the E_{chem} value resulted to be 3.14 eV, i.e., 0.6 eV stronger than the chemisorption of the first H atom. On the other hand, on singly hydrogenated anthracene, the *para* position is the only activated site. As expected, C atoms with local magnetic moment are also present at PAHs with different degree of hydrogenation; indeed, in studying the sequential hydrogenation of some PAHs it was recently observed that activated C atoms appear on hydrogenated PAHs presenting an odd number of extra H atoms [50], which result to be strongly reactive sites for subsequent hydrogenation reactions.
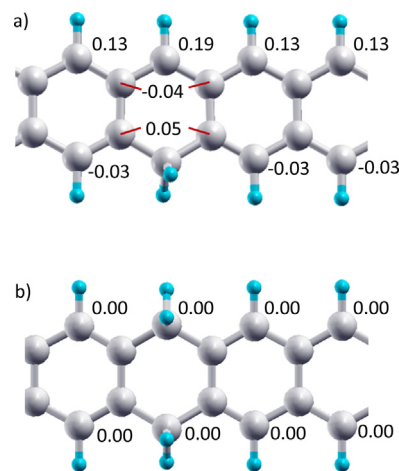
4. Conclusions

In this work, an infinite chain of polyacene was used as a model to analyze the electronic structure and reactivity of a zigzag edge of a relatively large PAH. In line with previous DFT calculations, we have found that the antiferromagnetic (AFM) phase of polyacene is more stable than the ferromagnetic (FM) one. A partial radical character on the edge C atoms appears in both cases, with higher spin values at the AFM phase ($0.11/−0.11$ μ_B).

The physisorption of atomic H on anthracene and polyacene was studied using a dispersion-corrected density functional theory (DFT-D) approximation, which is shown to perform satisfactorily in describing physisorption states. The minimal diffusion barriers from hollow to top sites were calculated in approximately 4 and 6 meV for anthracene and polyacene, respectively, for the most preferential channels.

In the sequential hydrogenation of PAHs, it was previously established from DFT calculations [18] that the addition of the first H atom to a peripheral C atom requires the highest barrier of all the process, calculated to be of about 60 meV on coronene. Our DFT results give essentially the same value for anthracene. On AFM polyacene, due to the partial radical character of their edge C atoms, the activation barrier is reduced to 34 meV. With DFT-D, the explicit incorporation of dispersion effects causes a reduction of the activation barrier with respect to the corresponding values with pure DFT. On the other hand, previous calculations performed using high-level ab initio methods [48] have demonstrated that on inner C atoms of PAHs, standard DFT tends to underestimate the activation barrier. Therefore, an even more pronounced reduction is expected with DFT-D. Thus, although pure DFT fails in describing properly the physisorption state, it seems to predict better results than DFT-D for the calculation of chemisorption barriers. In choosing the more

appropriated DFT implementation for studying the whole reaction profile, one faces a dilemma because DFT-D improves appreciably the physisorption well but predicts too low values for chemisorption barriers (at least with the original fitting of the parameters in the dispersion correction term).

The present results are of interest in the reaction of atomic hydrogen with PAHs at very low temperature conditions as the ones present in the cold interstellar medium. It was suggested that hydrogenated PAHs could act as efficient catalysts toward H_2 production in the interstellar medium. In this sense, we have found that relatively large PAHs with zigzag edges presenting partial radical character could be even more efficient reservoirs of atomic hydrogen than standard PAHs.

Acknowledgments

References

[1] F. Zereini, C.L.S. Wiseman (Eds.), Urban Airbone Particulate Matter, Springer-Verlag, Berlin, 2010.
[2] M. Rapacioli, F. Calvo, F. Spiegelman, C. Joblin, D.J. Wales, J. Phys. Chem. A 109 (2005) 2487.
[3] T.S. Totton, D. Chakrabarti, A.J. Misquitta, M. Sander, D.J. Wales, M. Kraft, Combust. Flame 157 (2010) 909.
[4] D.E. Jiang, B.G. Sumpter, S. Dai, J. Chem. Phys. 126 (2007) 134701.
[5] D.E. Jiang, B.G. Sumpter, S. Dai, J. Phys. Chem. B 110 (2006) 23628.
[6] A.J. Perez-Jimenez, J.C.S. Garcia, J. Am. Chem. Soc. 131 (2009) 14857.
[7] L.J. Allamandola, A.G.G.M. Tielen, J.R. Barker, ApJS 71 (1989) 733.
[8] V. Wakelam, E. Herbst, Astrophys. J. 680 (2008) 371.
[9] G. Vidali, Chem. Rev. 113 (2013) 8762.
[10] N. Rougeau, D. Teillet-Billy, V. Sidis, Phys. Chem. Chem. Phys. 13 (2011) 17579.
[11] X. Sha, B. Jackson, D. Lemoine, J. Chem. Phys. 116 (2002) 7158.
[12] Y. Ferro, F. Marinelli, A. Allouche, Chem. Phys. Lett. 368 (2003) 609.
[13] A.J.H.M. Meijer, A.J. Farebrother, D.C. Clary, A.J. Fisher, J. Phys. Chem. A 105 (2001) 2173.
[14] Y. Ferro, D. Teillet-Billy, N. Rougeau, V. Sidis, S. Morisset, A. Allouche, Phys. Rev. B 78 (2008) 085417.
[15] S. Casolo, R. Martinazzo, M. Bonfanti, G.F. Tantardini, J. Phys. Chem. A 113 (2009) 14545.
[16] J.D. Thrower, B. Jørgensen, E.E. Friis, S. Baouche, V. Mennella, A.C. Luntz, M. Andersen, B. Hammer, L. Hornekær, Astrophys. J. 752 (2012) 3.
[17] J. Szczepanski, J. Oomens, J.D. Steill, M.T. Vala, Astrophys. J. 727 (2011) 12.
[18] E. Rauls, L. Hornekær, Astrophys. J. 679 (2008) 531.
[19] J.A. Rasmussen, G. Henkelman, B. Hammer, J. Chem. Phys. 134 (2011) 164703.
[20] V. Mennella, L. Hornekær, J. Thrower, M. Accolla, Astrophys. J. 745 (2012) L2.
[21] M. Hirama, T. Tokosumi, T. Ishida, J. Aihara, Chem. Phys. 305 (2004) 307.
[22] Y. Fu, J. Szczepanski, N.C. Polfer, Astrophys. J. 744 (2012) 61.
[23] L. Boschman, G. Reitsma, S. Cazaux, T. Schlathölter, R. Hoekstra, M. Spaans, O. González-Magaña, Astrophys. J. 761 (2012) L33.
[24] M. Bonfanti, S. Casolo, G.F. Tantardini, A. Ponti, R. Martinazzo, J. Chem. Phys. 135 (2011) 164701.
[25] D.E. Jiang, S. Dai, J. Phys. Chem. A 112 (2008) 332.
[26] T. Wassmann, A.P. Seitsonen, A.M. Saitta, M. Lazzeri, F. Mauri, Phys. Rev. Lett. 101 (2008) 096402.
[27] D.E. Jiang, B.G. Sumpter, S. Dai, J. Chem. Phys. 127 (2007) 124703.
[28] F. Plasser, H. Pašalić, M.H. Gerzabek, F. Libisch, R. Reiter, J. Burgdörfer, T. Müller, R. Shepard, H. Lischka, Angew. Chem. Int. Ed. 52 (2013) 2581.
[29] H.F. Bettinger, Pure App. Chem. 82 (2010) 905.
[30] D.E. Jiang, X.Q. Chen, W. Luo, W.A. Shelton, Chem. Phys. Lett. 483 (2009) 120.
[31] S.F.M. Ashbourn, J.E. Elsila, J.P. Dworkin, M.P. Bernstein, S.A. Sandford, L.J. Allamandola, Meteorit. Planet. Sci. 42 (2007) 2035.
[32] J.L. Weisman, A. Mattioda, T.J. Lee, D.M. Hudgins, L.J. Allamandola, C.W. Bauschlicher Jr., M. Head-Gordon, Phys. Chem. Chem. Phys. 7 (2005) 109.
[33] G. Kresse, J. Hafner, Phys. Rev. B 47 (1993) 558.
[34] G. Kresse, J. Hafner, Phys. Rev. B 48 (1993) 13115.
[35] G. Kresse, J. Hafner, Phys. Rev. B 49 (1994) 14251.
[36] M.J. Frisch, Gaussian 03, Revision C.02, Gaussian, Inc., Wallingford, CT, 2004.
[37] S. Grimme, J. Comput. Chem. 27 (2006) 1787.
[38] M. Dion, H. Rydberg, E. Schröder, D.C. Langreth, B.I. Lundqvist, Phys. Rev. Lett. 92 (2004) 246401.
[39] J. Klimeš, D.R. Bowler, A. Michaelides, J. Phys.: Condens. Matter 22 (2010) 022201.
[40] G. Henkelman, B.P. Uberuaga, H.J. Jonsson, Chem. Phys. 113 (2000) 9901.
[41] S.F. Boys, F. Bernardi, Mol. Phys. 19 (1970) 553.
[42] M. Bonfanti, R. Martinazzo, G.F. Tantardini, A. Ponti, J. Phys. Chem. C 111 (2007) 5825.
[43] J. Ma, A. Michaelides, D. Alfè, J. Chem. Phys. 134 (2011) 134701.
[44] G.M. Psofogiannakis, G.E. Froudakis, J. Phys. Chem. C 113 (2009) 14908.
[45] R.M. Ferullo, N.F. Domancich, N.J. Castellani, Chem. Phys. Lett. 500 (2010) 283.
[46] M. Kocman, P. Jurečka, M. Dubecký, M. Otyepka, Y. Cho, K.S. Kim, Phys. Chem. Chem. Phys. 17 (2015) 6423.
[47] E.R.M. Davidson, J. Klimeš, D. Alfè, A. Michaelides, ACS Nano 8 (2014) 9905.
[48] Y. Wang, H.J. Qian, K. Morokuma, S. Irle, J. Phys. Chem. A 116 (2012) 7154.
[49] Y. Zhang, W. Yang, J. Chem. Phys. 109 (1998) 2604.
[50] B. Klærke, Y. Toker, D.B. Rahbek, L. Hornekær, L.H. Andersen, Astron. Astrophys. 549 (2013) A84.